Green Chemistry

PAPER

View Article Online
View Journal | View Issue

Cite this: *Green Chem.*, 2018, **20**, 4662

A bio-based route to the carbon-5 chemical glutaric acid and to bionylon-6,5 using metabolically engineered *Corynebacterium glutamicum*†

Christina Maria Rohles,[a] Lars Gläser,[a] Michael Kohlstedt,[a] Gideon Gießelmann,[a] Samuel Pearson,[b] Aránzazu del Campo,[b] Judith Becker[a] and Christoph Wittmann *[a]

Received 18th June 2018,
Accepted 16th August 2018

DOI: 10.1039/c8gc01901k

rsc.li/greenchem

In the present work, we established the bio-based production of glutarate, a carbon-5 dicarboxylic acid with recognized value for commercial plastics and other applications, using metabolically engineered *Corynebacterium glutamicum*. The mutant *C. glutamicum* AVA-2 served as a starting point for strain development, because it secreted small amounts of glutarate as a consequence of its engineered 5-aminovalerate pathway. Starting from AVA-2, we overexpressed 5-aminovalerate transaminase (*gabT*) and glutarate semialdehyde dehydrogenase (*gabD*) under the control of the constitutive *tuf* promoter to convert 5-aminovalerate further to glutarate. The created strain GTA-1 formed glutarate as a major product, but still secreted 5-aminovalerate as well. This bottleneck was tackled at the level of 5-aminovalerate re-import. The advanced strain GTA-4 overexpressed the newly discovered 5-aminovalerate importer NCgl0464 and formed glutarate from glucose in a yield of 0.27 mol mol^{-1}. In a fed-batch process, GTA-4 produced more than 90 g L^{-1} glutarate from glucose and molasses based sugars in a yield of up to 0.70 mol mol^{-1} and a maximum productivity of 1.8 g L^{-1} h^{-1}, while 5-aminovalerate was no longer secreted. The bio-based glutaric acid was purified to >99.9% purity. Interfacial polymerization and melt polymerization with hexamethylenediamine yielded bionylon-6,5, a polyamide with a unique structure.

Introduction

There is a rapid growth of interest to use renewables for the manufacture of sustainable chemicals and materials. In particular, bioplastics are promising products among the different bio-based sectors. At present, the bioplastics market grows between 20–100% per year and the production is expected to surpass six million tons in 2021. This trend explains the huge market potential assigned to bio-based chemicals, which can serve as building blocks for bioplastics, including dicarboxylic acids,[1–9] diamines[10–19] and diols.[20–24]

Glutaric acid (1,5-pentanedioic acid) is such an attractive building block for polymers.[25,26] It is used in the production of commercial polyesters and polyamides.[27] Moreover, it is built into organometallics, leading to antimicrobial agents,[28] transistors, and capacitors.[29] The dimethyl ester of glutaric acid is regarded as a green solvent and used as an ingredient in cleaning products, paints and coating formulations.[30] The hydrogenated form, 1,5-pentanediol,[31] is a monomer for polyesters and polyurethanes.[32] The costs and environmental concerns of traditional petrochemical routes to glutaric acid have stimulated research to produce this important chemical from renewable resources. Different approaches have demonstrated the production of glutarate and its derivative 5-aminovalerate.[26,33–35] However, glutarate titers have remained unattractively low so far. The most promising concepts to derive glutarate by fermentation build on L-lysine overproducing microbes,[25,26] previously engineered to accumulate the amino acid in high titers and yields.[36] Introducing the so-called aminovalerate pathway, L-lysine is converted into 5-aminovalerate by L-lysine 2-monooxygenase (DavB) and δ-aminovaleramidase (DavA) (Fig. 1A). The downstream glutarate pathway involves the enzymes aminobutyrate/aminovalerate aminotransferase (GabT) and succinate/glutarate semialdehyde dehydrogenase (GabD) to finally form glutarate. In *C. glutamicum*, these are encoded by the operons NCgl0462 (*gabT*) and NCgl0463 (*gabD*).[34] Using the L-lysine-mediated route, initial studies reported genetically modified *E. coli*,

[a]*Institute of Systems Biotechnology, Saarland University, Saarbrücken, Germany. E-mail: christoph.wittmann@uni-saarland.de; Tel: +49-(0) 681 302 71970*
[b]*Leibniz Institut für Neue Materialien, Saarbrücken, Germany*

†Electronic supplementary information (ESI) available. See DOI: 10.1039/c8gc01901k

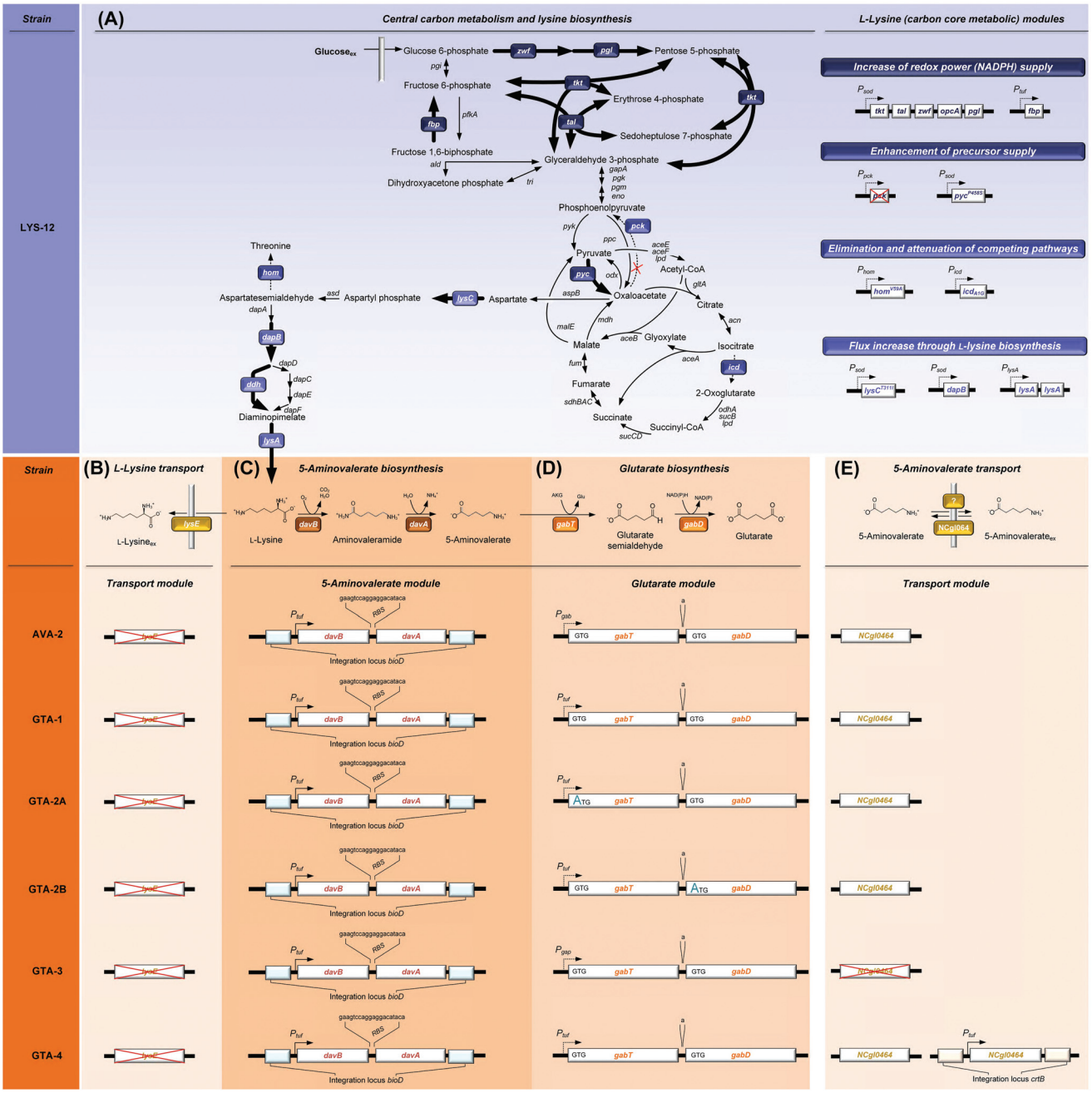

Fig. 1 Metabolic pathway design for the production of glutarate in *Corynebacterium glutamicum*. The overview illustrates the genomic layout of each producer, created in this work, including core carbon metabolism and L-lysine synthesis (A) and secretion (B), 5-aminovalerate synthesis (C), glutarate synthesis (D), and the newly discovered re-import of 5-aminovalerate (E). All modifications were implemented into the genome. The genes (*davBA*) from *P. putida* KT2440, encoding L-lysine monooxygenase (DavB) and 5-aminovaleramidase (DavA), were used to establish the 5-aminovalerate module. The two genes were integrated under the control of the constitutive *tuf*-promoter into the *bioD* locus of *C. glutamicum* LYS-12. LYS-12 comprised twelve genome-based modifications for lysine hyper production.[34] The glutarate module comprised 5-aminovalerate transaminase (GabT) and glutarate semialdehyde dehydrogenase (GabD), encoded by the native genes *gabTD*. Different variants of the modules were tested for optimization. The transport module comprised the L-lysine exporter *lysE* and the amino acid permease NCgl0464, expressed in its native form, deleted, and amplified *via* the genomic expression of a second gene copy in the *crtB* locus. The gene annotations for central metabolism and L-lysine synthesis are given in the ESI.†

which produced glutarate at a level of 0.8 g L^{-1} (ref. 25) and 1.7 g L^{-1}.[26] *E. coli* strains, engineered with a reverse adipate-degradation pathway, accumulated up to 4.8 g L^{-1} glutarate.[37] Another approach to glutarate recently suggested a bio-reduction of glutaconate, but is greatly limited by the supply of the precursor in the milligram range.[38] Likewise, glutarate bio-

synthesis *via* α-keto acid carbon chain extension and decarboxylation in recombinant *E. coli* has remained at titers of only 0.4 g L^{-1} until recently.[27]

C. glutamicum seems to be a most straightforward host to produce glutarate, because it is the major workhorse for the industrial manufacture of L-lysine,[39,40] a glutarate precursor. Different from other bacteria such as *E. coli*[25] and *P. putida*,[41,42] *C. glutamicum* does not degrade L-lysine, but retains the amino acid inside the cell upon deletion of the lysine exporter *lysE*,[34] preventing the loss of the precursor. From a metabolic viewpoint, the L-lysine-based pathway is the preferred route to make glutarate. It offers the highest theoretical yield (0.75 mol (mol glucose)$^{-1}$), higher than that of the alternative α-ketoglutarate-based synthesis (0.67 mol (mol glucose)$^{-1}$).[27] Despite these advantages, *C. glutamicum* has not been metabolically engineered so far to produce glutarate. It is even claimed that *C. glutamicum* has "serious limitations for glutarate production".[37] The fact that 5-aminovalerate-producing *C. glutamicum* strains accumulate glutarate as a by-product,[34,43] however, demonstrates the basic capability of the microbe to synthesize this interesting molecule.

Previously, our group has metabolically engineered *C. glutamicum* for the production of L-lysine,[36,44] ectoine,[45] diaminopentane,[14] and 5-aminovalerate,[34] all *via* the lysine route. Here, we describe systems metabolic engineering of *C. glutamicum* for high-level glutarate production. The recently developed producer *C. glutamicum* AVA-2 served as a starting point for strain engineering, because it exhibited an engineered aminovalerate pathway and excreted glutarate as a by-product in addition to 5-aminovalerate.[34] The advanced producer *C. glutamicum* GTA-4, obtained after several rounds of strain optimization, was evaluated in a fed-batch process. Subsequently, a strategy for down-stream purification was developed and applied to purify glutaric acid from fermentation. The obtained glutaric acid was used to derive bio-nylon-6,5.

Results and discussion

C. glutamicum can grow in the presence of up to 60 g L^{-1} glutarate

C. glutamicum could grow in the presence of up to 60 g L^{-1} glutarate (ESI, Fig. S1†). Increasing concentrations caused reduced growth rates, leading to a 50% growth reduction at a rather high glutarate concentration (K_I) of 46.0 ± 0.4 g L^{-1}. No growth was observed at 80 g L^{-1} glutarate. Similarly, the microbe also grew on agar plates up to a glutarate level of 60 g L^{-1}. *C. glutamicum* appeared significantly more tolerant than *E. coli*, already growth inhibited at 5 g L^{-1} glutarate and severely affected at 20 g L^{-1}.[25]

The overexpression of the 5-aminovalerate pathway module is not sufficient for selective glutarate production in *C. glutamicum*

During the growth of *C. glutamicum* AVA-2 on glucose as the sole source of carbon, 5-aminovalerate and glutarate were both secreted into the medium (Fig. 2A). The pathway precursor L-lysine was not secreted, resulting from the previously eliminated L-lysine exporter *lysE* in the genome of the AVA-2 strain.[34] The production of 5-aminovalerate and glutarate was growth-associated and stopped after the depletion of the substrate. With regard to a selective production of glutarate, the formation of 5-aminovalerate was undesired.

Overexpression of the native *gabTD* genes increases the glutarate production flux

To improve the glutarate production, we expressed the entire *gabTD* operon under the control of the strong constitutive *tuf*

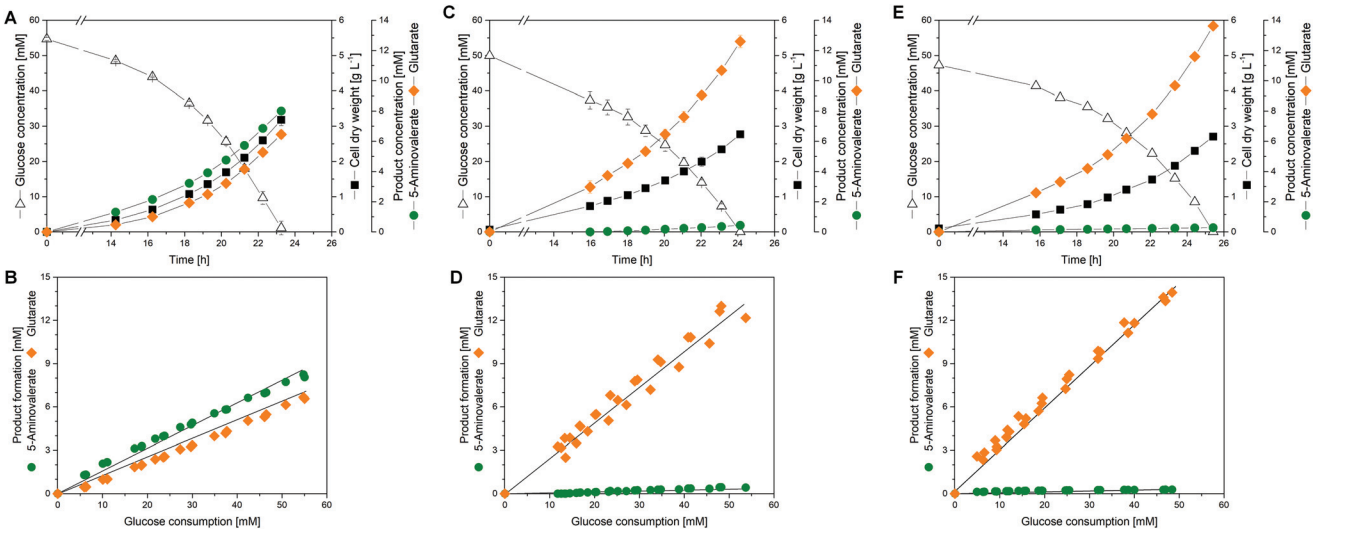

Fig. 2 Growth and production characteristics of glutarate producing *C. glutamicum* strains. The strains AVA-2 (A, B), GTA-1 (C, D), and GTA-4 (E, F) were cultivated in shake flasks at 30 °C in a chemically defined glucose medium. The cultivation profiles show growth, product formation, and glucose consumption over time (A, C, E) and yields (B, D, F). Error bars represent standard deviations from three biological replicates.

promoter (Fig. 1D). For this purpose, a 200 bp *tuf* promoter fragment was inserted into the genome upstream of the *gabTD* locus. Positive clones revealed a PCR fragment of 1.3 kb in contrast to the wild type (1.1 kB). After verification by sequencing, one clone was designated *C. glutamicum* GTA-1.

Cultured on glucose, GTA-1 accumulated 12.5 mM glutarate (Fig. 2C): 50% more than its ancestor AVA-2. Furthermore, the new mutant exhibited a twofold increased glutarate yield (265 ± 8 mmol mol^{-1}) and an eightfold reduced 5-aminovalerate production (Table 1 and Fig. 2D). The strong decrease in the 5-aminovalerate yield revealed that the major fraction of the precursor was successfully channeled to glutarate by the amplified glutarate module. As shown by enzymatic assays, the enhanced product yield benefited from a substantially enhanced activity of the pathway, which converted 5-aminovalerate to glutarate in two enzymatic steps (Fig. 1D). The GTA-1 strain revealed a 5 to 7-fold higher specific activity for 5-aminovalerate transaminase (159 mU mg^{-1}) and glutarate semialdehyde dehydrogenase (222 mU mg^{-1}) than the parent AVA-2 strain (GabT: 24 mU mg^{-1}, GabD: 42 mU mg^{-1}). The glutarate production was not further increased, when pyridoxal 5-phosphate (10 mg L^{-1}), a known cofactor for transaminases, was supplied to the cultivation medium (data not shown). Obviously, the endogenous supply of the vitamin was sufficient. Overall, the glutarate formation in GTA-1 made up 96% of the total production flux (Fig. 3).

Reinforcement of the glutarate pathway module at the level of translation upgrades the glutarate yield, but causes a decrease in cellular fitness

The genetic structure of the glutarate operon suggested a bicistronic transcript with individual translational start points for 5-aminovalerate transaminase (*gabT*) and glutarate semialdehyde dehydrogenase (*gabD*). The sequence further revealed that each of the genes contained the start codon GTG, previously found to be weak in translation efficiency.[46,47] To enhance translation, the GTG codon of the *gabT* gene was replaced by the stronger variant ATG. The obtained mutant *C. glutamicum* GTA-1 $gabT^{G1A}$, designated GTA-2A, revealed a shift of the product spectrum towards higher glutarate and lower 5-aminovalerate formation (Fig. 3), but suffered from 20% reduction of the specific growth rate (Table 1). In the same manner, the GTG codon in the *gabD* gene was replaced by ATG in the GTA-1 strain. The resulting mutant GTA-1 $gabD^{G1A}$ (GTA-2B) accumulated glutarate in a higher yield (Table 1 and Fig. 3), but also revealed an undesired decrease in fitness: its specific growth rate was reduced by almost 50% and the biomass yield was reduced by almost 20%, indicating undesired growth defects. This behavior was taken as an indication that the additional overexpression of only one of the two glutarate pathway genes was not the best approach to further enhance the pathway flux, so that the strains GTA-2A and GTA-2B were not considered further. Moreover, the remaining secretion of the by-product 5-aminovalerate was still an undesired feature.

Re-uptake of the secreted intermediate 5-aminovalerate contributes to glutarate formation

An isotope experiment was designed to study the 5-aminovalerate/glutarate metabolism in *C. glutamicum* in more detail and to identify further possibilities to improve production. Briefly, *C. glutamicum* AVA-2 was grown on minimal medium with 99% [$^{13}C_6$] glucose, additionally amended with naturally labeled 5-aminovalerate. An incubation without 5-aminovalerate served as a control. GC/MS analysis of the ^{13}C enrichment in glutarate, formed in the two set-ups, provided a direct readout, to which extent the external pathway intermediate was available for the metabolic conversion. When the non-labeled 5-aminovalerate had been added to the medium, the ^{13}C enrichment of glutarate was substantially reduced, as compared to the control (Table 2 and ESI Fig. S2†). The analysis revealed that 53% of glutarate was synthesized from glucose, whereas the remaining fraction (47%) stemmed from the externally supplied 5-aminovalerate. This feature appeared to be beneficial for production from glucose: secreted 5-aminovalerate was still available for the cells to be taken up and channeled to glutarate.

The obviously existing 5-aminovalerate importer protein, however, was not known. On a first glance, the amino acid permease NCgl0464 (*cgl0841*) appeared as a promising candidate, given its functional assignment to transport γ-amino butyrate,[50] which is structurally related to 5-aminovalerate. Moreover, the localization of NCgl0464 immediately downstream of the *gabTD* operon provided a reason to investigate its

Table 1 Growth and production performance of glutarate producing *C. glutamicum* strains during batch cultivation in shake flasks using a mineral salt medium with glucose as the sole carbon source. The data comprise the specific rates for growth (μ), glucose uptake (q_{Glc}), glutarate (q_{Glt}), and 5-aminovalerate formation (q_{Ava}). Additionally, the yields for biomass ($Y_{X/Glc}$), glutarate ($Y_{Glt/Glc}$), and 5-aminovalerate ($Y_{5\text{-}Ava/Glc}$) are given. Errors represent standard deviations from three biological replicates

	AVA-2	GTA-1	GTA-2A	GTA-2B	GTA-4
μ [h^{-1}]	0.22 ± 0.04	0.16 ± 0.00	0.14 ± 0.00	0.10 ± 0.00	0.18 ± 0.00
q_{Glc} [mmol g^{-1} h^{-1}]	4.6 ± 0.7	3.0 ± 0.1	2.8 ± 0.3	2.3 ± 0.1	3.3 ± 0.0
$q_{5\text{-}Ava}$ [mmol g^{-1} h^{-1}]	0.4 ± 0.1	0.1 ± 0.0	0.0 ± 0.0	0.0 ± 0.0	0.0 ± 0.0
q_{Glt} [mmol g^{-1} h^{-1}]	0.6 ± 0.1	0.8 ± 0.0	0.8 ± 0.0	0.7 ± 0.0	0.9 ± 0.0
$Y_{X/Glc}$ [g mol^{-1}]	47.6 ± 3.6	53.4 ± 4.0	49.4 ± 5.5	44.3 ± 1.6	54.3 ± 1.0
$Y_{5\text{-}Ava/Glc}$ [mmol mol^{-1}]	98 ± 2	12 ± 1	7 ± 3	14 ± 0	4 ± 0
$Y_{Glt/Glc}$ [mmol mol^{-1}]	123 ± 2	265 ± 8	277 ± 6	316 ± 5	271 ± 3

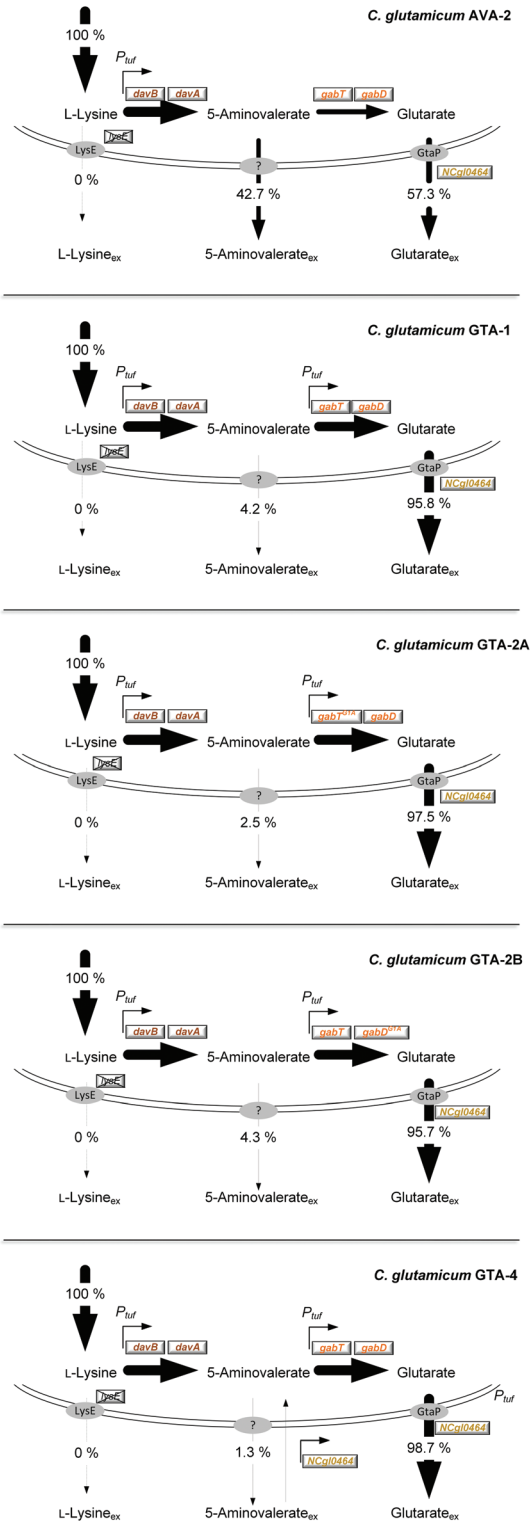

Fig. 3 Relative contribution of L-lysine, 5-aminovalerate and glutarate secretion to the overall production flux in *C. glutamicum* AVA-2, GTA-1, GTA-2A, GTA-2B and GTA-4. The production is given as a relative flux related to the overall L-lysine-based production flux, which was set to 100%.

Table 2 Labeling study of *C. glutamicum* for elucidation of its 5-aminovalerate/glutarate metabolism. The strains were grown in a mineral salt medium using [$^{13}C_6$]-labeled glucose with or without the addition of naturally labeled 5-aminovalerate (5-AVA). The ^{13}C enrichment in glutarate was assessed by GC-MS, raw data were then corrected for natural isotopes,[48] and the ^{13}C enrichment was obtained as summed fractional labeling (SFL).[49] Errors represent standard deviations from three replicates

Strain	Conditions	SFL
AVA-2	[$^{13}C_6$]-glucose	0.93 ± 0.00
AVA-2	[$^{13}C_6$]-glucose + 5-AVA	0.53 ± 0.00
GTA-3	[$^{13}C_6$]-glucose + 5-AVA	0.65 ± 0.00

role experimentally. First, the deletion of the NCgl0464 gene was realized in the parent AVA-2 producer. A positive clone, which revealed the desired PCR fragment of 1.2 kb and the correctly modified sequence, in contrast to the wild type (2.4 kb), was studied for its production characteristics. The ΔNCgl0464 mutant, designated GTA-3, revealed a substantially reduced re-cycling of external 5-aminovalerate (Table 2 and Fig. S1†). Only about 35% of glutarate stemmed from the re-uptake of 5-aminovalerate, while 65% was synthesized from glucose. In addition, the overall glutarate production was reduced (6 mM), while the 5-aminovalerate level was substantially increased (9 mM), which indicated that the protein NCgl0464 had 5-aminovalerate permease activity. The isotope data also demonstrated that *C. glutamicum* possesses one or more additional proteins besides NCgl0464 to import 5-aminovalerate. The fortification of 5-aminovalerate re-import emerged as a relevant metabolic engineering target.

The overexpression of the permease NCgl0464 enables almost exclusive glutarate production

The overexpression of the permease NCgl0464 was tackled by inserting a second gene copy under the control of the *tuf* promoter into the genome of the GTA-1 strain, the best performing strain in the constructed genealogy (Table 1 and Fig. 1E). Positive clones, which carried the desired second gene copy, were identified on the basis of a 2.4 kb PCR fragment, which contained the inserted sequence in contrast to the wild type (1.1 kb). The successful modification was further confirmed by sequencing. The new strain GTA-1 P_{tuf}*NCgl0464* was designated GTA-4. When tested in a shake flask in a batch culture, it exhibited improved performance and accumulated higher amounts of glutarate (Fig. 2E and F). In addition, GTA-4 formed the product in increased yield (271 mmol mol^{-1}) and productivity (0.9 mmol g^{-1} h^{-1}) (Table 1). The secretion of 5-aminovalerate was reduced by a factor of more than three, as compared to the GTA-1 strain, to a level of only about 1% of the glutarate formed (Fig. 3). Interestingly, the GTA-4 strain grew faster than its ancestor did. Regarding metabolic engineering, the transport of molecules across cell membranes is regarded crucial, although only relatively few successful cases are described.[13] So far, efforts have been focussed on the transport of the final product itself, to drive its excretion out of the

cell[13,51] or block its re-uptake.[52,53] In this regard our strategy, *i.e.* the amplification of a transport protein for enhanced re-assimilation of a pathway intermediate displays an interesting novel extension, which holds promising potential to be applied to other processes in biotechnology, often associated with the undesired secretion of valuable intermediates.

The cell factory *C. glutamicum* GTA-4 performs well under fed-batch conditions and accumulates more than 90 g L^{-1} of glutarate within 60 hours

To assess performance under industrially relevant conditions, we benchmarked the GTA-4 strain in a fed-batch process on a glucose-molasses medium (Fig. 4). During the initial batch phase, the strain grew exponentially (Fig. 4A) and accumulated glutarate in a yield of 0.28 mol mol^{-1} (Fig. 5). After 15 h, the initially supplied sugar (84 g L^{-1}) was depleted and the feed phase was started (Fig. 4A). Sucrose and fructose, contained at a lower level as molasses-based sugars (data not shown), were efficiently consumed during the first 8 hours and remained below the detection limit during the feed phase. In this way, *C. glutamicum*, equipped with efficient pathways to metabolize sucrose[54] and fructose,[55] handled the sugar mixture very well, including the high start concentration chosen. Pulses of the concentrated feed were automatically added, when the sugar was exhausted, which was nicely reflected by a sudden increase of the dissolved oxygen (DO) level (Fig. 4B). This correlation allowed a precise and robust control. Previous fermentations with *C. glutamicum* have shown that the microbe also performs well with other feed regimes such as linear ramps and pulse-wise additions, manually controlled using at-line monitoring of the sugar level.[14] The DO-based control chosen here, however, appears particularly robust and does not need external monitoring.[36,56] Further on, the glutarate level continuously increased from 15 g L^{-1} at the end of the batch phase to a final titer of more than 90 g L^{-1} after 60 hours. The cells produced glutarate exclusively, which provided a strong benefit for the subsequent down-stream processing (see below). The formation of 5-aminovalerate was negligible. A small amount, accumulating during the batch phase, was completely taken up again later (Fig. 4A). Other known by-products such as trehalose were not formed. The molar glutarate yield increased about 2.5-fold during the feed phase to 0.70 mol mol^{-1}, based on consumed sugar (Fig. 5). This value is nearly as high as the theoretical optimum of the pathway (0.75 mol mol^{-1}). Although a slight overestimation cannot be excluded, due to small amounts of yeast extract added (below 3/100 of sugar in feed) and certain levels of non-sugar compounds contained in

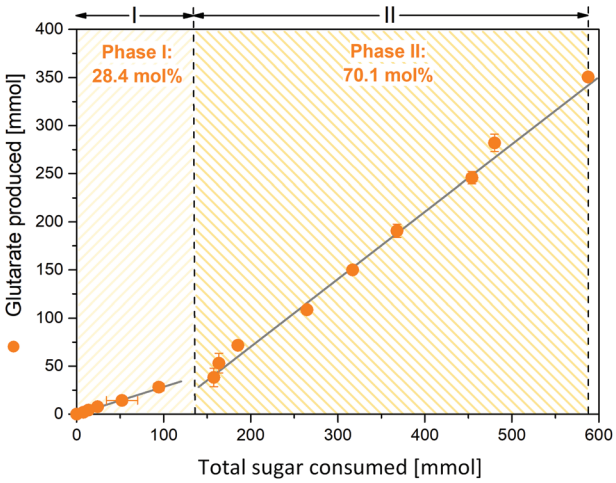

Fig. 5 Glutarate yield during fed-batch production by metabolically engineered *Corynebacterium glutamicum* GTA-4. The substrate is given as total sugar, *i.e.* the lumped concentration of glucose, sucrose, plus fructose, added as pure glucose or as molasses-based sugar (glucose, sucrose, fructose). The molar amount of the sugar reflects hexose units, *i.e.* one sucrose molecule in the mixture is considered as two hexoses (glucose plus fructose). The corresponding c-molar yields are obtained *via* multiplication of the molar yield values shown in the plot by a factor of 5/6: 0.24 c-mole c-$mole^{-1}$ (phase I), and 0.58 c-mole c-$mole^{-1}$ (phase II). The data represent mean values and deviations from two replicates.

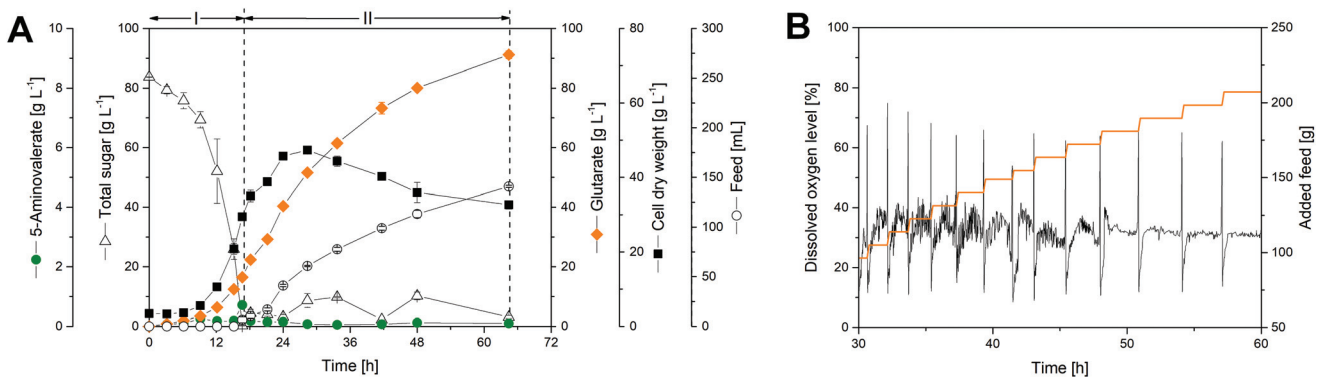

Fig. 4 Fed-batch production of glutarate by metabolically engineered *Corynebacterium glutamicum* GTA-4: culture profile (A), visualization of the automatic process control for a period of 30 hours during the feed phase (B). The substrate is given as total sugar, *i.e.* the lumped concentration of glucose, sucrose, plus fructose, either added as pure glucose or as molasses-based sugar (sucrose, glucose, fructose). After depletion of the initial sugar at the end of the batch phase, pulses of feed were added automatically, using an increase of the dissolved oxygen (DO) above 45% as a trigger. The data represent mean values and deviations from two replicates.

the molasses, the created cell factory exhibited an enormous synthetic selectivity. The space–time yield for glutarate was maximal during the feed phase (1.8 g L^{-1} h^{-1}). Averaged over the full process, production occurred at more than the half-maximum rate (1.4 g L^{-1} h^{-1}).

The increase in the glutarate yield was largely enabled by the systematically streamlined metabolism, which included 18 genomics traits that covered the entire route from the substrate to the product: the L-lysine module (12 genomic changes in 4 different carbon core metabolic modules) to drive L-lysine formation from sugar, the 5-aminovalerate module (2 genomic changes) to convert L-lysine into 5-aminovalerate, the glutarate module (2 genomic changes) to drive 5-aminovalerate further to glutarate, and the transport module (2 genomic changes) to optimize inflow and outflow of the pathway intermediates L-lysine and 5-aminovalerate (Fig. 1). In this way the substrate carbon, which became available during the feed phase, when the growth of the cells slowed down and later even ceased and the anabolic demand diminished, could be fully driven to the desired product in a yield close to the theoretical maximum. This demonstrates the power of systems metabolic engineering.[4,14,34,36,57–59] In addition, the performance benefited from a good robustness of *C. glutamicum*, which allowed cell growth up to about 60 g L^{-1} glutarate (ESI, Fig. S1†) and efficient product formation even at high glutarate levels, once growth slowed down or even stopped (Fig. 4A). Enabled by its systems-wide engineered metabolism and its native robustness, the GTA-4 strain accumulated twenty-fold more glutarate than any other microbe engineered so far.[37] Taken together, the developed strain provides glutarate in an attractive yield, titer and productivity and places the developed process into the high-level range of industrial bio-processes, using *C. glutamicum* for chemical production.[14,36,56]

Downstream processing of the fermentation broth provides bio-based glutaric acid with more than 99.9% purity

Following fermentation, glutaric acid was recovered from the culture broth by two-step acidification, vacuum evaporation, and crystallization (Fig. 6). After cell separation and pH adjustment to 2.5, the filtrate was concentrated in a vacuum evaporator, thereby precipitating significant fractions of inorganic salts. Crude glutaric acid was obtained by acidification to pH 1.0 and further volume reduction. The different acidification and concentration steps were found crucial to enable glutaric acid crystallization, likely due to the excellent solubility of this organic acid.[60] The crude crystals dissolved in acetone, while residual salts, insoluble in the solvent were separated by filtration. Recrystallization, washing and lyophilization, finally yielded a white crystalline powder. The product contained 98.2% pure glutaric acid with no organic impurities, but only traces of phosphate (ESI, Fig. S3A and B†). Alternative washing and recrystallization in chloroform provided the product at >99.9% purity (ESI, Fig. S3C and S4†). Nuclear magnetic resonance (NMR) spectroscopy showed no discernable difference to commercial glutaric acid (ESI, Fig. S5 and S6†).

Bio-based glutaric acid gives access to bio-polyamide PA6.5

Nylons are important industrial polymers displaying good temperature resistance, relatively high moduli, and excellent strength and toughness, but are produced almost exclusively from non-renewable feedstocks. Nylon-6,6, formed by the polycondensation of adipic acid and hexamethylene diamine, has the highest global production of all polyamides, and shows good all-round performance.[7,61] A greener route to nylon-6,6 *via* bio-adipic acid was recently reported[1,62–64] and reflects growing impetus to find renewable pathways to polyamides.[14,15,18,64] To demonstrate the potential of (bio-based) glutaric acid as a polyamide precursor, we successfully synthesized nylon-6,5 from the novel bio-based glutaric acid and from the commercial petrochemical for comparison. The interfacial polymerization (the nylon "rope trick") (Fig. 6) and the industrially relevant melt polymerization approaches (Fig. 5 and Fig. 7) were tested. The obtained polymers were analyzed by size exclusion chromatography (SEC) to determine their molar weight distribution. Thermal properties were character-

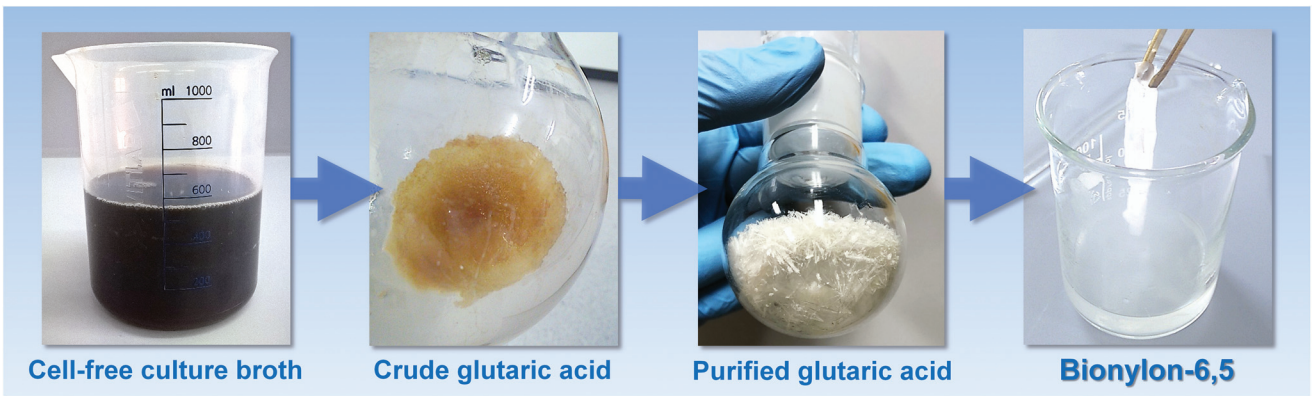

Fig. 6 Downstream purification of bio-based glutaric acid and polymerization into nylon-6,5. Crude glutaric acid was recovered from the broth by a two-step acidification and vacuum concentration procedure. Purified glutaric acid was obtained by crystallization. The bio-based glutaric acid was activated with oxalyl chloride and was then used to perform interfacial polycondensation with 1,6-hexamethylene diamine into nylon-6,5.

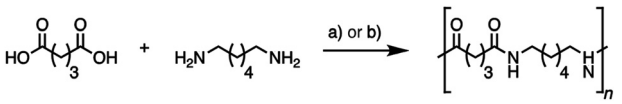

Fig. 7 Synthesis of nylon-6,5 by nylon "rope trick" interfacial polymerization *via* glutaryl chloride (a) and melt polymerization for 9 h under an inert atmosphere (b).

ized by differential scanning calorimetry (DSC) and thermogravimetric analysis (TGA).

All polymers showed similar characteristics (Table 3): molecular weights around 10.000 g mol^{-1}, polydispersity around 2.7 in interfacial polymerization and 1.8 in melt polymerization, melting temperature at 241–242 °C, crystallization enthalpy around 80 J g^{-1} and thermal stability up to 330 °C (ESI, Fig. S7, S8, and S9†). A small perturbation at the melting peak onset likely corresponded to the melting and recrystallization of a minor crystalline phase nylon-6,5. No significant differences were observed between the bio-based and the petrochemical based polymer. Bio-based glutaric acid is therefore a viable alternative to chemical glutaric acid for bioplastic synthesis, producing polymers of identical quality. The melt polymer molar masses are comparable to literature values for laboratory-scale melt-phase polyamide syntheses,[65] with higher values expected by increasing the reaction time and chain mobility by plasticization with water vapor throughout polymerization.[66] It seems that only one single study so far substantially studied nylon-6,5.[67] While reporting similar values for viscosity-average molar mass and melting point for their nylon-6,5 made by interfacial polymerization, the authors encountered the same minor endotherm at around 230 °C and attributed this phenomenon to polymer reorganization during heating of smaller crystalline domains, also observed for other nylons.[68] The unique structure of nylon-6,5 is a courtesy of its particular hydrogen bonding pattern, but other literature on nylon-6,5 is scarce, suggesting that its properties and potential applications remain largely unexplored. Nylons with fewer carbons per amide bond are more polar and therefore display higher water affinities. While increased water absorption can have unwanted plasticizing effects, more polar nylons can also offer advantages. Nylon-4 for example exhibits breathability, rivalling that of cotton due to its relatively high water affinity[69] and nylon-4,6 shows a particularly high crystallinity and melting point (>280 °C) due to a high density of hydrogen bonds.[70]

For future research, nylons with lower carbon to amide ratios are interesting materials in their own right, and glutaric acid is a prime candidate as a precursor for such polymers. Moreover, the novel production route, described here, opens sustainable alternatives to many other products, accessible from glutaric acid.

Conclusions

In this work, we established *C. glutamicum* as a production platform for the polymer building block glutaric acid through genome manipulation. As shown, we generated a strain with a highly attractive glutarate titer, yield and productivity. The created producer is fully genome based and offers genetic stability without the need for plasmids and antibiotic selection pressure, otherwise incompatible with industrial production. Recent claims that "*C. glutamicum* has serious limitations to produce glutarate"[37] should be revised: the GTA-4 strain accumulates twenty-fold more product than any other microbe engineered so far and displays a milestone towards bio-based glutarate production. Further optimization can be expected by additional rounds of strain analysis, design and genetic engineering,[71–74] which will leverage the performance further to industrial efficiency.[36,75–77] In addition to molasses, it appears feasible to use other raw materials also. *C. glutamicum* can be engineered to consume xylose, arabinose, and cellobiose,[78–81] which could open the use of lignocellulosic biomass to produce glutarate. Furthermore, the microbe has been recently upgraded to use mannitol, a major constituent of seaweed, which could fuel glutarate production with algal biomass from ocean farms in the future.[44] The bionylon-6,5 provides a promising addition to the portfolio of bio-based polyamides for future industrial applications.

Experimental

Microorganisms and plasmids

The ATCC 13032-derived *C. glutamicum* strain AVA-2[34] was used as a host to establish glutarate production. The wild type ATCC 13032 (American Type Culture Collection, Manassas, VA, USA)

Table 3 Thermal properties and molar mass characteristics of the nylon-6,5 polymers, produced from commercial glutaric acid of chemical origin and from bio-based glutaric acid, produced in this work *via* fermentation, using metabolically engineered *Corynebacterium glutamicum* GTA-4

Nylon-6,5 properties	Glutaric acid chemical	Glutaric acid biological	Glutaric acid chemical	Glutaric acid biological
Synthesis method	Interfacial polymerization	Interfacial polymerization	Melt polymerization	Melt polymerization
Glass transition temperature T_g (°C)	77	69	72	78
Melting temperature T_m (°C)	242	241	242	241
Enthalpy of crystallization ΔH_c (J g^{-1})	79	82	88	79
Number avg. molar mass M_n (g mol^{-1})	10 100	9900	11 300	10 800
Weight avg. molar mass M_w (g mol^{-1})	28 900	26 300	20 700	19 800
Dispersity	2.8	2.6	1.8	1.8

was used for tolerance testing. The amplification of transformation vectors on the basis of the integrative plasmid pClik int *sacB*[82,83] was carried out in the *Escherichia coli* strains DH5α and NM522 (Invitrogen, Carlsbad, CA, USA).[36] All strains and plasmids of this study are listed in Table 4.

Molecular design and genetic engineering

For molecular design, Clone Manager Professional 9 (Sci-Ed Software, Denver, USA) was used. The genetic construct for genome-based integration of the *tuf* promoter from *C. glutamicum*, upstream of the *gabT* (NCgl0462)/*gabD* (NCgl0463) operon, comprised (i) 500 bp-sized flanking regions as homologous recombination sites, and (ii) a 200 bp-sized DNA fragment of the promoter of the structural *tuf* gene (NCgl0480) (Fig. 1). The genetic construct for genome-based expression of a second copy of the permease NCgl0464 comprised (i) 500 bp-sized flanking regions as homologous recombination sites for the *crtB* locus (NCgl0598), and (ii) a 200 bp-sized DNA fragment of the promoter of the structural *tuf* gene (NCgl0480) and the permease gene NCgl0464 (Fig. 1). For a replacement of the translational start codon GTG by ATG in the *gabT* and the *gabD* gene, respectively, DNA fragments of 550 bp size were amplified upstream and downstream of the start codon of the corresponding gene, whereby the start codon exchange was implemented using modified primers. The amplification and assembly of DNA fragments and the amplification, purification and transformation of plasmid vectors into *E. coli* and *C. glutamicum* strains were performed as described previously.[34] PCR and sequence analysis (GATC Biotech AG, Konstanz, Germany) were used for plasmid and strain validation. Primer sequences are given in Table 5.

Batch cultivation in shake flasks

C. glutamicum was grown in baffled shake flasks with 10% filling volume at 30 °C and 230 rpm on an orbital shaker (Multitron, Infors AG, Bottmingen, Switzerland). The cultivation procedure involved one pre-culture in complex medium (37 g L^{-1} BHI, Becton Dickinson, Franklin Lakes, NJ, USA) followed by another pre-cultivation in minimal medium.[84] The main cultivation was carried out as triplicate in a chemically defined mineral salt medium with glucose as the carbon source.[47] The medium contained: (A) 500 mL of a salt stock (1 g NaCl, 55 mg $MgCl_2 \cdot 7H_2O$ and 200 mg $CaCl_2$), (B) 100 mL of a substrate stock (100 g L^{-1} glucose), (C) 100 mL of a buffer stock (2 M potassium phosphate, pH 7.8), (D) 100 mL of an ammonium stock (150 g L^{-1} $(NH_4)_2SO_4$, pH 7.0), (E) 20 mL of a vitamin stock (25 mg L^{-1} biotin, 50 mg L^{-1} thiamine·HCl, and 50 mg L^{-1} pantothenic acid), (F) 10 mL of an iron stock (2 g L^{-1} $FeSO_4$, pH 1.0), (G) 10 mL of a trace element stock,[85] (H) 1 mL of a DHB stock (30 mg mL^{-1} 3,4-dihydroxybenzoic acid in 0.3 M NaOH), and 159 mL deionized water. The stock solutions were sterilized by autoclaving (A–D), and by filtration (E–H), respectively, and combined at room temperature freshly before use.

Tolerance testing. *C. glutamicum* wild type was grown on a 1 mL scale in a micro bioreactor (BioLector I, m2plabs,

Table 4 *Corynebacterium glutamicum* strains and plasmids

Strain	Description	Ref.
AVA-2	Metabolically engineered producer of 5-aminovalerate and glutarate	34
GTA-1	AVA-2 + P_{tuf}*gabTD* encoding 5-aminovalerate transaminase (NCgl0462) and glutarate semialdehyde dehydrogenase (NCgl0463)	This work
GTA-2A	GTA-1 + $gabT^{G1A}$	This work
GTA-2B	GTA-1 + $gabD^{G1A}$	This work
GTA-3	AVA-2 + deletion of the amino acid permease gene NCgl0464	This work
GTA-4	GTA-1 + genome-based expression of a second copy of NCgl0464 under the control of the *tuf* promoter	This work

Plasmids	Description	Ref.
pTC	Expression vector for DNA methylation with ORI for *E. coli* and tetracycline resistance.	34
pClik int *sacB*	Integrative transformation vector for *C. glutamicum* with MCS, ORI for *E. coli*, and Kan^R and *sacB* as selection markers	82
pClik int *sacB* tuf_p-*gabTD*	Integrative transformation vector for insertion of the *tuf* promoter upstream of the *gabTD* operon	This work
pClik int *sacB* $gabT^{G1A}$	Integrative transformation vector for exchanging the start codon of *gabT* from GTG to ATG	This work
pClik int *sacB* $gabD^{G1A}$	Integrative transformation vector for exchanging the start codon of *gabD* from GTG to ATG	This work
pClik int *sacB* ΔNCgl0464	Integrative transformation vector for deletion of the amino acid permease NCgl0464	This work
pClik int *sacB* tuf_p-NCgl0464	Integrative vector for insertion of NCgl0464 under the control of the *tuf* promoter into the *crtB* locus	This work

Table 5 Primers for genome-based engineering of *C. glutamicum*

No.	Sequence	AT [°C]
$PR_{tuf\_gabTD}\_1$	CTGCGTTAATTAACAATTGGCGCTGGAGGTGATCGAGATAAATG	59
$PR_{tuf\_gabTD}\_2$	CATTCGCAGGGTAACGGCCAGGTTCCTCCTGTGAGGTGAGATAC	60
$PR_{tuf\_gabTD}\_3$	CTCACCTCACAGGAGGAACCTGGCCGTTACCCTGCGAATG	62
$PR_{tuf\_gabTD}\_4$	CGGTATGAGAGATCTTCCACTGTATGTCCTCCTGGACTTCGTG	60
$PR_{tuf\_gabTD}\_5$	GAAGTCCAGGAGGACATACAGTGGAAGATCTCTCATACCGC	57
$PR_{tuf\_gabTD}\_6$	AATCCCGGGTCTAGAGGATCCCGAATCCGGACTTGTATGG	57
$PR_{gabT\_G1A}\_1$	CTGCGTTAATTAACAATTGGTGCCAACGGATAAGACCACGCT	63
$PR_{gabT\_G1A}\_2$	ATCTTCCATTGTATGTCCTCCTGGACTTCGTGGT	69
$PR_{gabT\_G1A}\_3$	GACATACAATGGAAGATCTCTCATACCGCATCCC	68
$PR_{gabT\_G1A}\_4$	AATCCCGGGTCTAGAGGATCGGTTCTTCGCGGTCATCGCCAT	64
$PR_{gabD\_G1A}\_1$	CTGCGTTAATTAACAATTGGCCAGCGACGCAGAAGGTGTGAT	64
$PR_{gabD\_G1A}\_2$	GTCAAAGACATTTTAGCCCACCTTCTGGTGCG	68
$PR_{gabD\_G1A}\_3$	GTGGGCTAAAATGTCTTTGACCTTCCCAGTAATC	68
$PR_{gabD\_G1A}\_4$	AATCCCGGGTCTAGAGGATCTGAGACCAAGCCCTGCGGGATA	64
$PR_{\Delta NCgl0464}\_1$	CTGCGTTAATTAACAATTGGTCGCAGCTAACCGTTTCTTG	57
$PR_{\Delta NCgl0464}\_2$	GGAAGTGACTATGCCCAACCGTGCTGTACCTGCAGCATTG	58
$PR_{\Delta NCgl0464}\_3$	CAATGCTGCAGGTACAGCACGGTTGGGCATAGTCACTTCC	57
$PR_{\Delta NCgl0464}\_4$	AATCCCGGGTCTAGAGGATCAGGCGGTGAGCTGTACTTG	59
$PR_{tuf\_NCgl0464}\_1$	AATTGGGATCCTCTAGACCCGGTGGCTAGTCCTGCTAGTC	63
$PR_{tuf\_NCgl0464}\_2$	CATTCGCAGGGTAACGGCCACTCCTATGATCCGACTCAGTTG	61
$PR_{tuf\_NCgl0464}\_3$	CAACTGAGTCGGATCATAGGAGTGGCCGTTACCCTGCGAATG	67
$PR_{tuf\_NCgl0464}\_4$	GCAACTATTGATTCGGTAGTCATGTTGTATGTCCTCCTGGACTTC	60
$PR_{tuf\_NCgl0464}\_5$	GAAGTCCAGGAGGACATACAACATGACTACCGAATCAATAGTTGC	63
$PR_{tuf\_NCgl0464}\_6$	GAGTGGCCGATGAGGTTGTGGAAGTGACTATGCCCAACCC	63
$PR_{tuf\_NCgl0464}\_7$	GGGTTGGGCATAGTCACTTCCACAACCTCATCGGCCACTC	65
$PR_{tuf\_NCgl0464}\_8$	CCGCTAGCGATTTAAATCCCAGCACCAGTGACATTCCTTC	62

Baesweiler, Germany) using 48-well flower plates (MTP-48-B, m2plabs, Baesweiler, Germany) as described before.[56] The incubation in mineral salt medium, amended with different levels of glutarate (0, 20, 40, 60, 80 g L^{-1}), was conducted at 1300 rpm and 30 °C. Additionally, the tolerance to glutarate was monitored on a solid medium, composed of 37 g L^{-1} BHI, 15 g L^{-1} agar (Becton Dickinson), and different levels of glutarate (0, 20, 40, 60, 80 L^{-1}).

Fed-batch cultivation in stirred tank bioreactors

The production performance of the glutarate-producer *C. glutamicum* GTA-4 was evaluated in a fed-batch process. Fermentation was carried out in a glucose molasses medium using 1 L DASGIP bioreactors (Eppendorf, Jülich, Germany). The initial batch medium (300 mL), contained per liter: 72.4 g L^{-1} sugar cane molasses (Hansa Melasse, Bremen, Germany), 50 g L^{-1} glucose, 35 g L^{-1} yeast extract (Difco), 20 g L^{-1} $(NH_4)_2SO_4$, 100 mg L^{-1} $MgSO_4$, 60 mg L^{-1} Ca-pantothenate, 18 mg L^{-1} nicotinamide, 15 mg L^{-1} thiamine·HCl, 11 mg L^{-1} $FeSO_4{\cdot}7H_2O$, 10 mg L^{-1} citrate, 9 mg L^{-1} biotin, 250 µL H_3PO_4 (85%) and 5 mL Antifoam 204 (Sigma-Aldrich). The process was inoculated with exponentially growing cells from pre-cultures on BHI medium. Dissolved oxygen-based feeding (500 g L^{-1} glucose, 162.5 g L^{-1} sugar cane molasses, 40 g L^{-1} $(NH_4)_2SO_4$, 15 g L^{-1} yeast extract, 2 mL antifoam) was initiated, when the sugar concentration was depleted.

Feed shots of 5 mL were automatically added, when the dissolved oxygen level (pO_2) increased above 45%. Cultivation temperature and aeration rate were maintained constant at 30 °C and 1 vvm. The pH and the pO_2 level were monitored online with a pH electrode (Mettler Toledo, Gießen, Germany) and a pO_2 electrode (Hamilton, Höchst, Germany). The pH was kept constant at 7.0 ± 0.05 by automated addition of 10 M NaOH. The dissolved oxygen level was maintained above 30% of saturation by variation of stirrer speed and oxygen content in the gas inflow. Data acquisition and process operations were controlled by the DASGIP control software 4.0 (Eppendorf, Jülich, Germany).

Substrate and product quantification

Glucose, sucrose, fructose, trehalose, and organic acids including glutarate were separated by HPLC (Agilent 1260 Infinity Series, Agilent Technologies, Waldbronn, Germany) on an Aminex HPX-87H column (Bio-Rad, Hercules, California, USA) using 3.5 mM H_2SO_4 at 1 mL min^{-1} and 55 °C as the mobile phase. The analytes were quantified using refractive index detection (Agilent 1260 RID G1362A, Agilent Technologies) and external standards.

Amino acids and 5-aminovalerate were quantified by HPLC as described before.[34] The concentration of the cell dry mass (CDM) was calculated from the optical density, using a correlation factor of CDM [g L^{-1}] = 0.32 × OD_{660}.[34]

GC-MS analysis of glutaric acid

The labeling pattern of glutaric acid, obtained from the culture supernatant, was analyzed after derivatization into the *t*-butyl-dimethylsilyl derivative.[4] For this purpose, 10 µL culture supernatant was dried under a nitrogen stream, followed by incubation with 50 µL dimethylformamide (0.1% pyrimidine) and 50 µL methyl-*t*-butyldimethylsilyl-trifluoroacetamide (Macherey and Nagel, Düren, Germany) for 30 minutes at 80 °C. The obtained *t*-butyldimethylsilyl derivate was analyzed

by gas chromatography-mass spectrometry (GC-MS, 7890A, 5975C quadrupole detector, Agilent Technologies, Santa Clara, CA, USA).[86] For comparison, commercial glutaric acid was analyzed as a reference standard.

Determination of enzyme activities

Crude cell extracts were prepared from exponentially growing cells by mechanical cell disruption. A cultivation and harvest procedure was carried out as previously described.[34] Aliquots of 1 mL cell suspension were transferred into FastPrep-24 vials (MP Biomedicals, Illkirch-Graffenstaden, France) containing silica beads (Ø 0.1 mm). Cell disruption was carried out in 2 × 30 s cycles at 5000 rpm (Precellys-24, PeqLab, Hannover, Germany) including 1 minute cooling pauses on ice. Removal of cell debris and protein quantification was performed as previously described.[86] The activity of 5-aminovalerate transaminase was assayed in 50 mM Tris hydrochloride buffer (pH 8.5), additionally containing 2 mM 5-aminovalerate, 2 mM α-ketoglutarate, 50 mM KCl, 5 mM $MgCl_2$ 100 μM pyridoxal 5-phosphate, and crude cell extract (50 μL mL^{-1}). The reaction mixture was incubated at 30 °C. Samples were regularly taken and thermally inactivated (5 min, 100 °C). The consumption of 5-aminovalerate was quantified by HPLC as given above and used to calculate the specific enzyme activity. The GabD activity was assayed in 100 mM Tris/HCl buffer (pH 8.5), additionally containing 100 mM KCl, 10 mM $MgCl_2$, 2 mM glutarate semialdehyde, and 0.5 mM NAD. The formation of NADH was monitored online at 340 nm and used for activity calculation ($\varepsilon_{340,NADH}$ = 6.22 L $mmol^{-1}$ cm^{-1}). Negative controls were conducted without the addition of crude cell extract and substrate, respectively.

Glutaric acid recovery and purification

After biomass separation *via* centrifugation (10 min, 8500*g*, 4 °C), the fermentation supernatant was vacuum-filtered (Whatman filter paper, Grade 3, Sigma-Aldrich). The pH of the filtrate was adjusted to pH 2.5, using 37% HCl, followed by volume reduction to about 30% in a vacuum concentrator (15 mbar, 40 °C, 1200 rpm, Christ, Germany). Precipitated inorganic salts were removed (Whatman filter paper, Grade 3, Sigma-Aldrich) and the obtained concentrate was incubated for 1 h with 5% (w/vol) activated carbon. After removal of the activated carbon (Whatman filter paper, Grade 3, Sigma-Aldrich), glutaric acid was crystallized by acidification to pH 1.0 with 85% H_3PO_4, a further volume reduction to about 10% of the initial volume, and incubation at 4 °C.

The obtained crude crystals were dissolved in acetone, while insoluble salts were separated *via* vacuum filtration (regenerated cellulose, 0.45 μm, Sartorius). After evaporation of the acetone, the obtained crystals were washed with deionized water and were then lyophilized (Christ Gefriertrocknungsanlagen, Osterode am Harz, Germany), which yielded a white crystalline powder. Alternatively, re-crystallization was conducted using chloroform. The purity of glutaric acid was assessed by GC-MS, as described above.

Synthesis of nylon-6,5 by interfacial polymerization

A stock solution of glutaryl chloride was prepared by suspending glutaric acid (1.60 g, 12.1 mmol, 1 equiv.) in a commercial oxalyl chloride solution (2.0 M in dichloromethane (DCM), 13.3 mL, 26.6 mmol, 2.2 equiv.) under nitrogen and adding dry dimethylformamide (DMF, 50 μL) as a catalyst. A bubbler was fitted, and the suspension was stirred at r.t. for 1 h, at which point bubbling had ceased and the reaction was complete. The DCM and unreacted oxalyl chloride were removed under vacuum. The residue was re-dissolved in dry DCM (24.2 mL) under nitrogen to give a 0.5 M solution. 1,6-Hexamethylene diamine (HMDA, 0.352 g, 3.03 mmol, 1 equiv.) was dissolved in 0.5 M NaOH (6.1 mL) to give 0.5 M HMDA.

For polymerization, a portion of glutaryl chloride stock solution (6.1 mL, 3.0 mmol, 1 equiv.) was transferred to a small beaker, and the HMDA solution was carefully added on top to avoid phase mixing. The polymer, formed at the interface of the two solutions, was taken with tweezers, and was wound around a glass stirring rod to generate a nylon rope. The resulting nylon-6,5 was washed with deionized water and vacuum dried before characterization.

Synthesis of nylon-6,5 by melt polymerization

Hexamethylene diamine (5.419 g, 46.6 mmol) was dissolved in water (1.35 mL) and a solution of glutaric acid (6.161 g, 46.6 mmol) in water (5.5 mL) was added dropwise with stirring in an ice bath. The resulting nylon-6,5 salt was precipitated in 2-propanol (200 mL) with vigorous stirring, isolated by vacuum filtration, and dried under vacuum. The salt was loaded into a 50 mL Schlenk flask, along with extra HMDA (0.02 equiv.) and a stir bar. The flask was heated to 170 °C in an oil bath under a gentle nitrogen flow for 1.5 h, by which time the reaction medium solidified. The flask was cooled to room temperature, and the solid was crushed with a spatula before heating at 210 °C under vacuum (20 mbar) for a further 7.5 h.

Polymer characterization

Size exclusion chromatography was performed with an 1260 Infinity system (Agilent), equipped with a Polymer Standards Service mixed bed column (PSS SDV linear S + 5 μm, separation range 100–150 000 g mol^{-1}) as a stationary phase, THF at 24 °C and a flow rate of 1 mL min^{-1} as a mobile phase, and a RID detector. Calibration was conducted with PMMA standards at 1 mg mL^{-1} (M_p = 602, 2160, 5980, 12 900, 22 800, 41 400, and 88 500 g mol^{-1}). Prior to the analysis, the nylon samples were functionalized overnight with trifluoroacetic anhydride in dry dichloromethane (DCM) to render them soluble. After drying, they were re-dissolved in dry THF at 2 mg mL^{-1} for analysis.

Thermogravimetric analysis was performed on an STA Jupiter 449 F 3 analyzer (Netzsch, Germany) under an argon atmosphere. A sample of about 5 mg was weighed into an aluminum crucible, and was then heated from room temperature to 600 °C at a rate of 5 °C min^{-1}. Differential scanning calorimetry (DSC) was performed on a Mettler Toledo DSC 1 (Gießen, Germany) under an argon atmosphere. A sample of

about 5 mg was weighed into an aluminum crucible, and was then analyzed by consecutive heating and cooling cycles between 0 °C and 280 °C, with 5 min isotherms between each ramp. After an initial heating and cooling cycle at 20 °C min^{-1} to erase the thermal history, the glass transition temperature (T_g) and melting temperature (T_m) were determined by heating the sample at a rate of 20 °C min^{-1}, and the enthalpy of crystallization (ΔH_c) was determined using a cooling rate of 20 °C min^{-1}. Thermograms were analyzed using STARe (Mettler Toledo) software.

Conflicts of interest

There are no conflicts to declare.

Acknowledgements

The authors acknowledge the excellent assistance of Michel Fritz, Robert Drumm, and the INM analysis department for the analytics.

References

1 M. Kohlstedt, S. Starck, N. Barton, J. Stolzenberger, M. Selzer, K. Mehlmann, R. Schneider, D. Pleissner, J. Rinkel, J. S. Dickschat, J. Venus, J. B. J. H. van Duuren and C. Wittmann, *Metab. Eng.*, 2018, **47**, 279–293.
2 N. Barton, L. Horbal, S. Starck, M. Kohlstedt, A. Luzhetskyy and C. Wittmann, *Metab. Eng.*, 2018, **45**, 200–2010.
3 J. Becker, A. Lange, J. Fabarius and C. Wittmann, *Curr. Opin. Biotechnol*, 2015, **36**, 168–175.
4 J. Becker, J. Reinefeld, R. Stellmacher, R. Schäfer, A. Lange, H. Meyer, M. Lalk, O. Zelder, G. von Abendroth, H. Schröder, S. Haefner and C. Wittmann, *Biotechnol. Bioeng.*, 2013, **110**, 3013–3023.
5 B. J. Harder, K. Bettenbrock and S. Klamt, *Metab. Eng.*, 2016, **38**, 29–37.
6 S. Okino, R. Noburyu, M. Suda, T. Jojima, M. Inui and H. Yukawa, *Appl. Microbiol. Biotechnol.*, 2008, **81**, 459–464.
7 D. R. Vardon, N. A. Rorrer, D. Salvachua, A. E. Settle, C. W. Johnson, M. J. Menart, N. S. Cleveland, P. N. Ciesielski, K. X. Steirer, J. R. Dorgan and G. T. Beckham, *Green Chem.*, 2016, **18**, 3397–3413.
8 Y. Tsuge, T. Hasunuma and A. Kondo, *J. Ind. Microbiol. Biotechnol.*, 2015, **42**, 375–389.
9 J. M. Otero, D. Cimini, K. R. Patil, S. G. Poulsen, L. Olsson and J. Nielsen, *PLoS One*, 2013, **8**, e54144.
10 J. Schneider and V. F. Wendisch, *Appl. Microbiol. Biotechnol.*, 2010, **88**, 859–868.
11 S. Kind, W. K. Jeong, H. Schröder and C. Wittmann, *Metab. Eng.*, 2010, **12**, 341–351.
12 S. Kind, W. K. Jeong, H. Schröder, O. Zelder and C. Wittmann, *Appl. Environ. Microbiol.*, 2010, **76**, 5175–5180.
13 S. Kind, S. Kreye and C. Wittmann, *Metab. Eng.*, 2011, **13**, 617–627.
14 S. Kind, S. Neubauer, J. Becker, M. Yamamoto, M. Völkert, G. V. Abendroth, O. Zelder and C. Wittmann, *Metab. Eng.*, 2014, **25**, 113–123.
15 S. Kind and C. Wittmann, *Appl. Microbiol. Biotechnol.*, 2011, **91**, 1287–1296.
16 Z. G. Qian, X. X. Xia and S. Y. Lee, *Biotechnol. Bioeng.*, 2009, **104**, 651–662.
17 Z. G. Qian, X. X. Xia and S. Y. Lee, *Biotechnol. Bioeng.*, 2011, **108**, 93–103.
18 K. Imao, R. Konishi, M. Kishida, Y. Hirata, S. Segawa, N. Adachi, R. Matsuura, Y. Tsuge, T. Matsumoto, T. Tanaka and A. Kondo, *Bioresour. Technol.*, 2017, **245**, 1684–1691.
19 N. Ikeda, M. Miyamoto, N. Adachi, M. Nakano, T. Tanaka and A. Kondo, *AMB Express*, 2013, **3**, 67.
20 N. E. Altaras and D. C. Cameron, *Appl. Environ. Microbiol.*, 1999, **65**, 1180–1185.
21 E. Celinska, *Biotechnol. Adv.*, 2010, **28**, 519–530.
22 D. Rados, A. L. Carvalho, S. Wieschalka, A. R. Neves, B. Blombach, B. J. Eikmanns and H. Santos, *Microb. Cell Fact.*, 2015, **14**, 171.
23 H. Yim, R. Haselbeck, W. Niu, C. Pujol-Baxley, A. Burgard, J. Boldt, J. Khandurina, J. D. Trawick, R. E. Osterhout, R. Stephen, J. Estadilla, S. Teisan, H. B. Schreyer, S. Andrae, T. H. Yang, S. Y. Lee, M. J. Burk and S. Van Dien, *Nat. Chem. Biol.*, 2011, **7**, 445–452.
24 S. Niimi, N. Suzuki, M. Inui and H. Yukawa, *Appl. Microbiol. Biotechnol.*, 2011, **90**, 1721–1729.
25 J. Adkins, J. Jordan and D. R. Nielsen, *Biotechnol. Bioeng.*, 2013, **110**, 1726–1734.
26 S. J. Park, E. Y. Kim, W. Noh, H. M. Park, Y. H. Oh, S. H. Lee, B. K. Song, J. Jegal and S. Y. Lee, *Metab. Eng.*, 2013, **16**, 42–47.
27 J. Wang, Y. Wu, X. Sun, Q. Yuan and Y. Yan, *ACS Synth. Biol.*, 2017, **6**, 1922–1930.
28 S. W. Jaros, M. F. Guedes da Silva, M. Florek, P. Smolenski, A. J. Pombeiro and A. M. Kirillov, *Inorg. Chem.*, 2016, **55**, 5886–5894.
29 A. F. Baldwin, R. Ma, A. Mannodi-Kanakkithodi, T. D. Huan, C. Wang, M. Tefferi, J. E. Marszalek, M. Cakmak, Y. Cao, R. Ramprasad and G. A. Sotzing, *Adv. Mater.*, 2015, **27**, 346–351.
30 S. Trivedi, D. Fluck, A. Sehgal, A. Osborne, M. S. Dahanayake, R. Talingting-Pabalan, J. Ruiz and C. Aymes, *US* 8222194B2, 2008.
31 H. Nagahara, M. Ono and K. Nakagawa, *JP* S6485937A, 1987.
32 J. Lu, L. Wu and B. G. Li, *ACS Sustainable Chem. Eng.*, 2017, **5**, 6159–6166.
33 S. J. Park, Y. H. Oh, W. Noh, H. Y. Kim, J. H. Shin, E. G. Lee, S. Lee, Y. David, M. G. Baylon, B. K. Song, J. Jegal, S. Y. Lee and S. H. Lee, *Biotechnol. J.*, 2014, **9**, 1322–1328.
34 C. M. Rohles, G. Giesselmann, M. Kohlstedt, C. Wittmann and J. Becker, *Microb. Cell Fact.*, 2016, **15**, 154.
35 P. Liu, H. Zhang, M. Lv, M. Hu, Z. Li, C. Gao, P. Xu and C. Ma, *Sci. Rep.*, 2014, **4**, 5657.

36 J. Becker, O. Zelder, S. Haefner, H. Schröder and C. Wittmann, *Metab. Eng.*, 2011, **13**, 159–168.
37 M. Zhao, G. Li and Y. Deng, *Appl. Environ. Microbiol.*, 2018, **84**(16), e00814-18.
38 I. Djurdjevic, O. Zelder and W. Buckel, *Appl. Environ. Microbiol.*, 2011, **77**, 320–322.
39 J. Becker and C. Wittmann, *Curr. Opin. Biotechnol.*, 2012, **23**, 718–726.
40 L. Eggeling and M. Bott, *Appl. Microbiol. Biotechnol.*, 2015, **99**, 3387–3394.
41 O. Revelles, M. Espinosa-Urgel, T. Fuhrer, U. Sauer and J. L. Ramos, *J Bacteriol.*, 2005, **87**, 7500–7510.
42 J. P. Vandecasteele and M. Hermann, *Eur. J. Biochem.*, 1972, **31**, 80–85.
43 J. H. Shin, S. H. Park, Y. H. Oh, J. W. Choi, M. H. Lee, J. S. Cho, K. J. Jeong, J. C. Joo, J. Yu, S. J. Park and S. Y. Lee, *Microb. Cell Fact.*, 2016, **15**, 174.
44 S. L. Hoffmann, L. Jungmann, S. Schiefelbein, L. Peyriga, E. Cahoreau, J. C. Portais, J. Becker and C. Wittmann, *Metab. Eng.*, 2018, **47**, 475–487.
45 J. Becker, R. Schäfer, M. Kohlstedt, B. J. Harder, N. S. Borchert, N. Stöveken, E. Bremer and C. Wittmann, *Microb. Cell Fact.*, 2013, **12**, 110.
46 J. Becker, N. Buschke, R. Bücker and C. Wittmann, *Eng. Life Sci.*, 2010, **10**, 430–438.
47 J. Becker, C. Klopprogge, H. Schröder and C. Wittmann, *Appl. Environ. Microbiol.*, 2009, **75**, 7866–7869.
48 W. A. van Winden, C. Wittmann, E. Heinzle and J. J. Heijnen, *Biotechnol. Bioeng.*, 2002, **80**, 477–479.
49 C. Wittmann, *Microb. Cell Fact.*, 2007, **6**, 6.
50 Z. Zhao, J. Y. Ding, W. H. Ma, N. Y. Zhou and S. J. Liu, *Appl. Environ. Microbiol.*, 2012, **78**, 2596–2601.
51 M. Li, D. Li, Y. Huang, M. Liu, H. Wang, Q. Tang and F. Lu, *J. Ind. Microbiol. Biotechnol.*, 2014, **41**, 701–709.
52 X. Xie, L. Xu, J. Shi, Q. Xu and N. Chen, *J. Ind. Microbiol. Biotechnol.*, 2012, **39**, 1549–1556.
53 Y. Li, H. Cong, B. Liu, J. Song, X. Sun, J. Zhang and Q. Yang, *Antonie van Leeuwenhoek*, 2016, **109**, 1185–1197.
54 C. Wittmann, P. Kiefer and O. Zelder, *Appl. Environ. Microbiol.*, 2004, **70**, 7277–7287.
55 P. Kiefer, E. Heinzle, O. Zelder and C. Wittmann, *Appl. Environ. Microbiol.*, 2004, **70**, 229–239.
56 J. Becker, M. Kuhl, M. Kohlstedt, S. Starck and C. Wittmann, *Microb. Cell Fact.*, 2018, **17**, 115.
57 A. L. Rodrigues, J. Becker, A. O. de Souza Lima, L. M. Porto and C. Wittmann, *Biotechnol. Bioeng.*, 2014, **111**, 2280–2289.
58 I. Poblete-Castro, D. Binger, A. Rodrigues, J. Becker, V. A. Martins Dos Santos and C. Wittmann, *Metab. Eng.*, 2013, **15**, 113–123.
59 A. L. Rodrigues, N. Trachtmann, J. Becker, A. F. Lohanatha, J. Blotenberg, C. J. Bolten, C. Korneli, A. O. de Souza Lima, L. M. Porto, G. A. Sprenger and C. Wittmann, *Metab. Eng.*, 2013, **20**, 29–41.
60 M. Z. H. Rozaini and P. Brimblecombe, *J. Chem. Thermodyn.*, 2009, **41**, 980–983.
61 C. W. Johnson, D. Salvachua, P. Khanna, H. Smith, D. J. Peterson and G. T. Beckham, *Metab. Eng. Commun.*, 2016, **3**, 111–119.
62 D. R. Vardon, M. A. Franden, C. W. Johnson, E. M. Karp, M. T. Guarnieri, J. G. Linger, M. J. Salm, T. J. Strathmann and G. T. Beckham, *Energy Environ. Sci.*, 2015, **8**, 617–628.
63 C. W. Johnson, P. E. Abraham, J. G. Linger, P. Khanna, R. L. Hettich and G. T. Beckham, *Metab. Eng. Commun.*, 2017, **5**, 19–25.
64 T. Polen, M. Spelberg and M. Bott, *J. Biotechnol.*, 2013, **167**, 75–84.
65 O. Turunc, M. Firdaus, G. Klein and M. A. R. Meier, *Green Chem.*, 2012, **14**, 2577–2583.
66 E. Roerdink and J. M. M. Warnier, *Polymer*, 1985, **26**, 1582–1588.
67 E. Navarro, L. Franco, J. A. Subirana and J. Puiggali, *Macromolecules*, 1995, **28**, 8742–8750.
68 C. Millot, L. A. Fillot, O. Lame, P. Sotta and R. Seguela, *J. Therm. Anal. Calorim.*, 2015, **122**, 307–314.
69 K.-S. Kang, Y.-K. Hong, Y. J. Kim and J. H. Kim, *Fibers Polym.*, 2014, **15**, 1343–1348.
70 E. Roerdink and J. M. M. Warnier, *Polymer*, 1985, **26**(10), 1582–1588.
71 J. Nielsen, *Annu. Rev. Biochem.*, 2017, **86**, 245–275.
72 K. Campbell, J. Xia and J. Nielsen, *Trends Biotechnol.*, 2017, **35**, 1156–1168.
73 M. D. Lynch, *Curr. Opin. Biotechnol.*, 2016, **38**, 106–111.
74 A. Lange, J. Becker, D. Schulze, E. Cahoreau, J.-C. Portais, S. Haefner, H. Schröder, J. Krawczyk, O. Zelder and C. Wittmann, *Metab. Eng.*, 2017, **44**, 198–212.
75 S. Y. Lee and J. H. Park, *Adv. Biochem. Eng./Biotechnol.*, 2010, **120**, 1–19.
76 J. Becker and C. Wittmann, *Curr. Opin. Microbiol.*, 2018, **45**, 180–188.
77 J. Ohnishi, S. Mitsuhashi, M. Hayashi, S. Ando, H. Yokoi, K. Ochiai and M. Ikeda, *Appl. Microbiol. Biotechnol.*, 2002, **58**, 217–223.
78 H. Kawaguchi, A. A. Vertes, S. Okino, M. Inui and H. Yukawa, *Appl. Environ. Microbiol.*, 2006, **72**, 3418–3428.
79 S. S. Yim, J. W. Choi, S. H. Lee and K. J. Jeong, *ACS Synth. Biol.*, 2016, **5**, 334–343.
80 N. Buschke, H. Schröder and C. Wittmann, *Biotechnol. J.*, 2011, **6**, 306–317.
81 M. Sasaki, T. Jojima, H. Kawaguchi, M. Inui and H. Yukawa, *Appl. Microbiol. Biotechnol.*, 2009, **85**, 105–115.
82 J. Becker, C. Klopprogge, O. Zelder, E. Heinzle and C. Wittmann, *Appl. Environ. Microbiol.*, 2005, **71**, 8587–8596.
83 S. Kind, J. Becker and C. Wittmann, *Metab. Eng.*, 2013, **15**, 184–195.
84 J. Becker, C. Klopprogge and C. Wittmann, *Microb. Cell Fact.*, 2008, **7**, 8.
85 J. J. Vallino and G. Stephanopoulos, *Biotechnol. Bioeng.*, 1993, **41**, 633–646.
86 N. Buschke, J. Becker, R. Schäfer, P. Kiefer, R. Biedendieck and C. Wittmann, *Biotechnol. J.*, 2013, **8**, 557–570.

